

1 **An *Escherichia coli* nitrogen starvation response is important**
2 **for mutualistic coexistence with *Rhodopseudomonas palustris***

3 Alexandra L. McCully¹, Megan G. Behringer², Jennifer R. Gliessman¹, Evgeny V. Pilipenko³ Jeffrey L.
4 Mazny¹, Michael Lynch², D. Allan Drummond³, James B. McKinlay^{1#}

5
6 ¹Department of Biology, Indiana University, Bloomington, IN

7 ²School of Life Sciences; Biodesign Center for Mechanisms of Evolution, Arizona State University,
8 Tempe, AZ.

9 ³Department of Biochemistry & Molecular Biology; Department of Human Genetics, University of
10 Chicago, Chicago IL.

11
12
13 Running title (54 max): Nitrogen starvation response in a bacterial mutualism

14 #Corresponding author. 1001 E 3rd Street, Jordan Hall, Bloomington, IN 47405

15 Phone: 812-855-0359

16 Email: jmckinla@indiana.edu

17 **Conflict of interest.**

18 The authors declare no conflict of interest

19 **Abstract (250)**

20 Microbial mutualistic cross-feeding interactions are ubiquitous and can drive important community
21 functions. Engaging in cross-feeding undoubtedly affects the physiology and metabolism of individual
22 species involved. However, the nature in which an individual's physiology is influenced by cross-feeding
23 and the importance of those physiological changes for the mutualism have received little attention. We
24 previously developed a genetically tractable coculture to study bacterial mutualisms. The coculture
25 consists of fermentative *Escherichia coli* and phototrophic *Rhodospseudomonas palustris*. In this
26 coculture, *E. coli* anaerobically ferments sugars into excreted organic acids as a carbon source for *R.*
27 *palustris*. In return, a genetically-engineered *R. palustris* constitutively converts N_2 into NH_4^+ , providing
28 *E. coli* with essential nitrogen. Using RNA-seq and proteomics, we identified transcript and protein levels
29 that differ in each partner when grown in coculture versus monoculture. When in coculture with *R.*
30 *palustris*, *E. coli* gene expression changes resembled a nitrogen starvation response under the control of
31 the transcriptional regulator NtrC. By genetically disrupting *E. coli* NtrC, we determined that a nitrogen
32 starvation response is important for a stable coexistence, especially at low *R. palustris* NH_4^+ excretion
33 levels. Destabilization of the nitrogen starvation regulatory network resulted in population heterogeneity
34 and in some cases, extinction. Our results highlight that alternative physiological states can be important
35 for survival within cooperative cross-feeding relationships.

36

37 **Importance (150)**

38 Mutualistic cross-feeding between microbes within multispecies communities is widespread. Studying
39 how mutualistic interactions influence the physiology of each species involved is important for
40 understanding how mutualisms function and persist in both natural and applied settings. Using a bacterial
41 mutualism consisting of *Rhodospseudomonas palustris* and *Escherichia coli* growing cooperatively
42 through bidirectional nutrient exchange, we determined that an *E. coli* nitrogen starvation response is
43 important for maintaining a stable coexistence. The lack of an *E. coli* nitrogen starvation response
44 ultimately destabilized the mutualism and, in some cases, led to community collapse after serial transfers.

45 Our findings thus inform on the potential necessity of an alternative physiological state for mutualistic
46 coexistence with another species compared to the physiology of species grown in isolation.

47

48 **Introduction**

49 Within diverse microbial communities, species engage in nutrient cross-feeding with reciprocating
50 partners as a survival strategy (1). In cases where species are not obligate mutualists, transitioning from a
51 free-living lifestyle to one based on cross-feeding can change the physiological state of the cells involved,
52 the extent to which depends on the nature of the cross-feeding relationship. For example, cross-feeding
53 can promote physiological changes that increase virulence (2, 3) or drastically alter cellular metabolism
54 (4), in some cases allowing for lifestyles that are only possible during mutualistic growth with a partner
55 (4–7). Aside from these examples, relatively little is known about how cell physiology is influenced by
56 mutualistic cross-feeding, despite the prevalence of cross-feeding in microbial communities.

57 Synthetic communities, or cocultures, are ideally suited for studying the physiological responses
58 to cooperative cross-feeding given their tractability (8, 9). We previously developed a bacterial coculture
59 that consists of fermentative *Escherichia coli* and the N₂-fixing photoheterotroph *Rhodospseudomonas*
60 *palustris* (Fig. 1) (10). In this coculture, *E. coli* anaerobically ferments glucose into organic acids,
61 providing *R. palustris* with essential carbon. In return, a genetically engineered *R. palustris* strain (Nx)
62 constitutively fixes N₂ gas, resulting in NH₄⁺ excretion that provides *E. coli* with essential nitrogen. The
63 result is an obligate mutualism that maintains a stable coexistence and reproducible growth trends (10) as
64 long as bidirectional nutrient cross-feeding levels are maintained within a defined range (11, 12).

65 Here we determined how nutrient cross-feeding between *E. coli* and *R. palustris* Nx alters the
66 physiological state of each partner population. Using RNA-seq and proteomic analyses, we identified
67 genes in both species that were differentially expressed in coculture compared to monoculture, with *E.*
68 *coli* exhibiting more overall changes in gene expression than *R. palustris* Nx. Specifically, *E. coli* gene
69 expression patterns resembled that of nitrogen-deprived cells, as many upregulated genes were within the
70 nitrogen starvation response regulon, controlled by the master transcriptional regulator NtrC. Genetic

71 disruption of *E. coli ntrC* resulted in variable growth trends at low *R. palustris* NH_4^+ excretion levels and
72 prevented long-term mutualistic coexistence with *R. palustris* across serial transfers. Our results highlight
73 the fact that cross-feeding relationships can stimulate alternative physiological states for at least one of
74 the partners involved and that adjusting cell physiology to these alternative states can be critical for
75 maintaining coexistence.

76

77 **Results**

78 **Engaging in an obligate mutualism alters the physiology of cooperating partners.** In our coculture, *E.*
79 *coli* and *R. palustris* Nx carry out complementary anaerobic metabolic processes whose products serve as
80 essential nutrients for the respective partner. Specifically, *E. coli* ferments glucose into acetate, lactate,
81 and succinate, which serve as carbon sources for *R. palustris* Nx, while other fermentation products such
82 as formate and ethanol accumulate; in return *R. palustris* Nx fixes N_2 and excretes NH_4^+ as the nitrogen
83 source for *E. coli* (Fig. 1). We previously demonstrated that our coculture supports a stable coexistence
84 and exhibits reproducible growth and metabolic trends when started from a wide range of starting species
85 ratios, including single colonies (10). However, we hypothesized that coculture conditions affected the
86 physiology of each species, particularly *E. coli*, based on the following observations. First, as growth is
87 coupled in our coculture, *E. coli* is forced to grow 4.6-times slower in coculture with *R. palustris* Nx than
88 it does in monoculture with abundant NH_4^+ , and its growth is restrained to only 10% of the population
89 (10). In contrast, *R. palustris* Nx grows at a rate in coculture that is comparable to that in monoculture
90 (12), consuming a mixed pool of excreted organic acids from *E. coli*. Second, coculturing pulls *E. coli*
91 fermentation forward due to removal of inhibitory end products. Indeed, we observed higher yields of
92 formate, an *E. coli* fermentation product that *R. palustris* does not consume, in cocultures compared to *E.*
93 *coli* monocultures (10).

94 To determine changes in gene expression patterns imposed by coculturing, we performed RNA-
95 seq and comparative proteomic analyses (13) on exponential phase cocultures and monocultures of *E. coli*
96 and *R. palustris* Nx. To make direct comparisons, all cultures were grown in the same basal anaerobic

97 minimal medium and monocultures were supplemented with the required carbon or nitrogen sources to
98 permit growth for each species. Cocultures and *E. coli* monocultures were provided glucose as a sole
99 carbon source, whereas a mixture of organic acids and bicarbonate was provided to *R. palustris* Nx
100 monocultures, as *R. palustris* does not consume glucose. For a nitrogen source, all cultures were grown
101 under a N₂ headspace, and *E. coli* monocultures were further supplemented with NH₄Cl, as *E. coli* is
102 incapable of using N₂. We identified several differentially expressed genes between monoculture and
103 coculture conditions in both species with more differences observed in *E. coli* compared to *R. palustris*
104 Nx, in agreement with our initial hypothesis (Fig. 2). For *E. coli*, out of 4377 ORFs, 55 were upregulated
105 and 68 were downregulated (Table 1) (log₂ value cutoff=2). Out of 4836 ORFs in *R. palustris* Nx, 14
106 were upregulated and 20 were downregulated (Table 1) (log₂ value cutoff=2). We also considered that
107 due to lower *E. coli* abundance in coculture, the apparently larger *E. coli* gene response may be partly due
108 to decreased resolution and thus increased error variance. Reassuringly, many of the genes identified as
109 being differentially expressed by RNA-seq were in agreement with the proteomic results (Table 2). Both
110 RNA-seq and proteomic analyses identified the *E. coli* ammonium transporter AmtB as an important,
111 upregulated gene in coculture, corroborating our previous findings that *E. coli* AmtB activity is important
112 for stable coexistence with *R. palustris* (12). Many *E. coli* genes involved in amino acid and purine
113 biosynthesis were downregulated in coculture (Table 1, Table 2), consistent with the lower observed
114 growth rate. Additionally, many *E. coli* flagellar and chemotaxis proteins were downregulated in
115 coculture (Table 1, Table 2), perhaps suggesting that motility is not important for coculture growth.
116 Alternatively, lower flagellar and chemotaxis transcript levels could be part of a general stress response
117 (14), perhaps associated with nitrogen limitation in cocultures. Whereas many of the differentially
118 expressed *E. coli* genes have been characterized in the literature, the *R. palustris* genes showing the
119 largest differential expression were uncharacterized genes encoding upregulated putative
120 alcohol/aldehyde dehydrogenases and a downregulated putative TonB-dependent receptor/siderophore
121 (Table 1, Table 2). Together, these datasets provide insight on how engaging in obligate cross-feeding
122 changes the lifestyle of each partner.

123

124 **An *E. coli* nitrogen starvation response is important for mutualistic growth with *R. palustris*.** We

125 chose to further examine differential gene expression patterns in *E. coli* as its growth rate and

126 fermentation profile are drastically affected by coculturing, whereas the *R. palustris* Nx growth rate is

127 similar to that in monoculture. We identified several *E. coli* genes and proteins that were upregulated in

128 coculture with *R. palustris* Nx compared to monoculture growth (Table 1, Table 2). We hypothesized that

129 the deletion of highly upregulated *E. coli* genes would negatively affect its growth in coculture. We made

130 deletions in *E. coli* genes that were identified in both RNA-seq and proteome datasets as well as the

131 highest upregulated *E. coli* transcript (*rutA*). We did not examine the effect of deleting *amtB* in this case

132 as we previously determined it to be important for coculture growth (12). These selected *E. coli* genes

133 were all involved in metabolism of alternative nitrogen sources such as D-ala-D-ala dipeptides (*ddpX*,

134 *ddpA*) (15), pyrimidines (*rutA*) (16), amino acids (*argT*) (17), and polyamines (*patA*, *potF*) (18). In

135 monocultures with 15mM NH₄Cl, there were negligible differences in growth or fermentation profiles

136 between WT *E. coli* or any of the single deletion mutants (Fig. S1). These results are consistent with

137 findings by others, as these genes are only important when scavenging alternative nitrogen sources that

138 are not present in our defined medium. We next tested these *E. coli* mutants in coculture to test if these

139 genes were important when NH₄⁺ is slowly cross-fed from *R. palustris* Nx. In all cocultures of *E. coli*

140 mutants paired with *R. palustris* Nx, there were no differences in the coculture growth curves (Fig. 3A) or

141 the final cell densities of each species (Fig. 3B). Additionally, there were no significant differences in the

142 growth rates, growth yields, or product yields from cocultures containing the *E. coli* mutants (Fig. S2).

143 These data suggest that none of these highly expressed *E. coli* genes are solely important for coculture

144 growth. While it is possible that synergistic expression of these genes is important for *E. coli*'s lifestyle in

145 coculture, the actual nitrogen sources accessed by expression of these genes are absent in the defined

146 medium. Thus, unless *E. coli* gains access to alternative nitrogen sources that we are unaware of in

147 coculture with *R. palustris* Nx, synergistic expression of these genes likely provides little to no benefit.

148 Even though individual deletions of the *E. coli* genes showing high expression in coculture had
149 no effect on coculture trends, we noted that they were all involved in nitrogen scavenging and fell within
150 the regulon of the transcription factor, NtrC, which controls the nitrogen starvation response (19). During
151 nitrogen limitation, the sensor kinase NtrB phosphorylates the response regulator NtrC (19).
152 Phosphorylated NtrC then binds to DNA and activates expression of ~45 genes (20), including those we
153 tested genetically above and *amtB*, which we previously determined to be important for coculture growth
154 (12). To examine the importance of the *E. coli* nitrogen starvation response in coculture, we deleted *ntrC*.
155 We first checked for any general defects of the resulting Δ NtrC mutant in monoculture with 15 mM
156 NH_4Cl and found that it exhibited similar growth and metabolic trends to WT *E. coli* (Fig. S3). We then
157 paired *E. coli* Δ NtrC with *R. palustris* Nx in coculture. Compared to cocultures using WT *E. coli*,
158 cocultures with *E. coli* Δ NtrC exhibited slower growth rates, longer lag periods (Fig. 4A), and lower final
159 *E. coli* cell densities (Fig. 4D). The long lag phase was less prominent in starter cocultures inoculated
160 from single colonies (Fig. S4A) compared to test cocultures inoculated with a 1% dilution of the starter
161 cocultures (Fig. 4A). This result suggests that starting *E. coli* Δ NtrC cocultures from single colonies
162 stimulated early growth, perhaps by increasing the *E. coli* frequency to be similar to that of *R. palustris*
163 when started with colonies of similar sizes rather than a dilution of stationary cocultures wherein the *E.*
164 *coli* frequency was low (~0.1%; Fig. 4D). A higher initial *E. coli* frequency might help *E. coli* acquire
165 excreted NH_4^+ before it is taken back up by *R. palustris* cells and thereby promote reciprocal cross-
166 feeding, similar to what we observed previously in cocultures with *E. coli* Δ AmtB mutants that were
167 defective for NH_4^+ uptake (12).

168 The overall coculture metabolism was also altered when *E. coli* Δ NtrC was paired with *R.*
169 *palustris* Nx. In cocultures pairing WT *E. coli* with *R. palustris* Nx, glucose is typically fully consumed
170 within 5 days coinciding with the accumulation of formate and ethanol (10). Cocultures pairing *E. coli*
171 Δ NtrC with *R. palustris* Nx differed in this regard, leaving ~40% of the glucose unconsumed after 10
172 days and exhibiting little to no formate and ethanol accumulation (Fig. S4B). Even despite the lower
173 glucose consumption, the final *R. palustris* cell density of cocultures pairing *R. palustris* Nx with *E. coli*

174 Δ NtrC was similar to those with WT *E. coli*. This unexpectedly high cell density could be explained by
175 consumption of formate and ethanol by *R. palustris* Nx, though we have never observed consumption of
176 formate by *R. palustris* Nx in monoculture. Alternatively, a lack of formate and/or ethanol production by
177 *E. coli* could explain the high cell density if the fermentation profile were shifted towards organic acids
178 that *R. palustris* normally consumes, namely acetate, lactate and succinate. Together, these data indicate
179 that misregulation of the nitrogen starvation response affected coculture growth and metabolism.

180 As noted above, the low *E. coli* Δ NtrC population and decreased coculture growth rate when
181 paired with *R. palustris* Nx resembled trends from cocultures that contained *E. coli* Δ AmtB mutants (12).
182 We previously found that the *E. coli* NH_4^+ transporter, AmtB, was required for coexistence with *R.*
183 *palustris* Nx across serial transfers as the transporter gives *E. coli* a competitive advantage in acquiring
184 the transiently available NH_4^+ before it can be reclaimed by the *R. palustris* population (12). To determine
185 if *E. coli* Δ NtrC was capable of maintaining a stable coexistence in coculture, we inoculated cocultures of
186 *E. coli* Δ NtrC paired with *R. palustris* Nx at equivalent CFUs and performed serial transfers every 10
187 days. While average final *E. coli* frequencies were consistently between 0.6 – 2.8 % (Fig. 5A), the values
188 became variable across serial transfers, as did coculture growth rates, lag periods, and net changes in both
189 *E. coli* and *R. palustris* cell densities (Fig. 5). This variability was due to 2 of the 4 lineages exhibiting
190 improved coculture growth over successive transfers (Fig. 5B,C), perhaps due to the emergence of
191 compensatory mutations, while the other two lineages showed declining growth trends (Fig. 5D,E).
192 Indeed, by transfers 5 and 6 there was little to no coculture growth in the slower-growing lineages (Fig
193 4D,E). The heterogeneity in growth trends through of serial transfers of cocultures with *E. coli* Δ NtrC is
194 in stark contrast to the stability of cocultures with WT *E. coli*, which we have serially transferred over 100
195 times with no extinction events (McKinlay, unpublished data). The nitrogen starvation response thus
196 appears to be important for long-term survival of the mutualism.

197

198 **Increased NH_4^+ cross-feeding levels can compensate for the absence of a nitrogen starvation**
199 **response.** The NtrC regulon is critical during periods of nitrogen starvation, activating a wide variety of

200 genes that are important for scavenging diverse nitrogen sources (20). We hypothesized that higher *R.*
201 *palustris* NH_4^+ cross-feeding levels could mitigate the poor growth of *E. coli* ΔNtrC in coculture by
202 making the nitrogen starvation response less important for survival. Previously, we engineered an *R.*
203 *palustris* Nx strain that excretes 3-times more NH_4^+ by deleting *R. palustris* NH_4^+ transporters encoded by
204 *amtB1* and *amtB2* (Nx Δ AmtB) (10). N_2 -fixing bacteria use AmtB to reacquire NH_4^+ that leaks outside the
205 cell, and Δ AmtB mutants thus accumulate NH_4^+ into the supernatant (10, 12, 21). In agreement with our
206 hypothesis, cocultures with *R. palustris* Nx Δ AmtB exhibited similar growth trends regardless of the *E.*
207 *coli* strain used (Fig. 4B,D). As *R. palustris* Nx Δ AmtB excretes more NH_4^+ than *R. palustris* Nx, it was
208 previously shown to result in faster WT *E. coli* growth and subsequent fermentation rates in coculture,
209 ultimately leading to the accumulation of consumable organic acids (Fig. S4B) and acidification of the
210 medium, inhibiting *R. palustris* growth (10). Cocultures pairing *R. palustris* Nx Δ AmtB and *E. coli* ΔNtrC
211 similarly exhibited growth (Fig. 4B,D), and fermentation profile trends (Fig. S4B) that were
212 indistinguishable from cocultures pairing *R. palustris* Nx Δ AmtB with WT *E. coli*. These similar trends
213 indicate that high *R. palustris* NH_4^+ excretion can eliminate the trends observed when the *E. coli* nitrogen
214 starvation response is compromised due to a ΔNtrC mutation.

215 One possibility for why high NH_4^+ cross-feeding levels eliminate the need for *E. coli* *ntrC* is that
216 the free NH_4^+ levels might be sufficiently high enough to prevent activation of the *E. coli* NtrC regulon.
217 However, comparative RNA-seq and proteomic analyses revealed that the same *E. coli* genes within the
218 NtrC regulon that were highly upregulated in cocultures pairing WT *E. coli* with *R. palustris* Nx were
219 also upregulated in cocultures with *R. palustris* Nx Δ AmtB (Table 1, Table 2). Thus, even though the *E.*
220 *coli* nitrogen starvation response is activated when cocultured with *R. palustris* Nx Δ AmtB, this response
221 is likely dispensable if there is sufficiently high NH_4^+ cross-feeding.

222

223 ***E. coli* NtrC is required for adequate AmtB expression to access cross-fed NH_4^+ in coculture.** While
224 a high level of *R. palustris* NH_4^+ excretion can compensate for an improper *E. coli* nitrogen starvation
225 response, less NH_4^+ excretion could potentially exaggerate problems emerging from the absence of NtrC.

226 We previously constructed an *R. palustris* Δ AmtB strain that excreted 1/3rd of the NH_4^+ than *R. palustris*
227 Nx in monoculture and which could not coexist in coculture with *R. palustris* Δ AmtB (12). The reason for
228 this lack of coexistence was due to *R. palustris* Δ AmtB outcompeting *E. coli* Δ AmtB for the lower level
229 of transiently available NH_4^+ , thus limiting *E. coli* growth and thereby the reciprocal supply of
230 fermentation products to *R. palustris* (12). Expression of *E. coli* *amtB* is thus important in coculture in
231 order to maintain coexistence. Indeed, RNA-seq and proteomic analyses revealed that *E. coli* AmtB
232 transcript and protein levels were upregulated in all cocultures pairing WT *E. coli* with any of the three *R.*
233 *palustris* strains (Nx, Nx Δ AmtB, Δ AmtB) (Table 1, Table 2). We thus wondered whether *E. coli* Δ NtrC
234 would coexist with the low NH_4^+ -excreting strain *R. palustris* Δ AmtB in coculture, as *E. coli* *amtB*
235 expression is transcriptionally activated by NtrC. Consistent with our previous findings, *R. palustris*
236 Δ AmtB supported a high relative WT *E. coli* population in coculture (Fig. 4D) (12). When cocultured
237 with WT *E. coli*, *R. palustris* Δ AmtB responds to NH_4^+ loss to *E. coli* by upregulating nitrogenase activity
238 since it has a wild-type copy of NifA (12). As a result, *R. palustris* Δ AmtB cross-feeds enough NH_4^+ to
239 stimulate a high WT *E. coli* frequency and subsequent accumulation of consumable organic acids, similar
240 to cocultures with *R. palustris* Nx Δ AmtB (Fig 3D, Fig. S4B) (12). In contrast, when we paired *E. coli*
241 Δ NtrC with *R. palustris* Δ AmtB, little to no coculture growth was observed (Fig. 4C), similar to previous
242 observations in cocultures pairing *E. coli* Δ AmtB with *R. palustris* Δ AmtB (12). Starter cocultures
243 inoculated with single colonies of each species in this pairing grew to low cell densities (Fig. S4A), and
244 test cocultures inoculated from these starter cocultures resulted in little to no growth, even after prolonged
245 incubation (Fig. 4C).

246 As AmtB is under the control of NtrC (20), we hypothesized that cocultures pairing *E. coli* Δ NtrC
247 with *R. palustris* Δ AmtB resulted in insufficient *E. coli* *amtB* expression, leading to poor competition for
248 NH_4^+ , which *R. palustris* will require if given the chance (12). We thus predicted that increased
249 expression of *amtB* in *E. coli* Δ NtrC would result in increased net growth of both species, as *E. coli*
250 Δ NtrC would be more competitive for essential NH_4^+ and be able to grow and produce more organic acids

251 for *R. palustris* Δ AmtB. To test this prediction, we obtained a plasmid harboring an IPTG-inducible copy
252 of *amtB* (*pamtB*) for use in *E. coli* Δ NtrC. AmtB is typically tightly regulated and only expressed when
253 NH_4^+ concentrations are below 20 μM , as cells acquire sufficient NH_4^+ through passive diffusion of NH_3
254 across the membrane at higher concentrations (22). Additionally, excessive NH_4^+ uptake through AmtB
255 transporters that exceeds the rate of assimilation can result in a futile cycle, as excess NH_3 inevitably
256 diffuses outside the cell (19). We first tested the effect of *pamtB* in WT *E. coli* monocultures with 15 mM
257 NH_4Cl . Induction with 1 mM IPTG prevented growth whereas 0.1 mM IPTG permitted growth albeit at a
258 decreased growth rate (Fig. S5). We thus decided to use 0.1 mM IPTG to induce *amtB* expression in all
259 cocultures described below. In cocultures pairing *E. coli* Δ NtrC *pamtB* with *R. palustris* Δ AmtB, more
260 growth was observed than in cocultures with *E. coli* Δ NtrC harboring an empty vector (pEV) (Fig. 6A). In
261 cocultures with *E. coli* Δ NtrC pEV, the *R. palustris* Δ AmtB cell density increased whereas the *E. coli* cell
262 density did not (Fig. 6B). The *R. palustris* growth was likely due to growth-independent cross-feeding of
263 fermentation products from *E. coli* maintenance metabolism, a phenomenon we described previously
264 (11). In contrast, cell densities of both species increased in cocultures pairing *R. palustris* Δ AmtB with *E.*
265 *coli* Δ NtrC *pamtB* (Fig. 6C), in agreement with our hypothesis that poor *E. coli* *amtB* expression
266 contributed to the lack of growth in this coculture pairing. Thus, while we cannot rule out that other genes
267 within the *E. coli* *ntrC* regulon are not important for coculture growth, the necessity of NtrC to upregulate
268 *amtB* is clearly important.

269

270 Discussion

271 In this study, we found that reciprocal nutrient cross-feeding between *E. coli* and *R. palustris* resulted in
272 significant changes in gene expression in both species compared to monocultures. Based on the RNA-seq
273 and proteomic analyses, we determined that *E. coli* alters its physiology to adopt a nitrogen-starved state
274 in response to low NH_4^+ cross-feeding levels from *R. palustris*. We subsequently determined that this
275 nitrogen-starved state is important for coexistence as genetic elimination of the master transcriptional
276 regulator, NtrC, resulted in variable population outcomes. Mutualistic nutrient cross-feeding has also been

277 shown to change the lifestyle of interacting partners in other systems. In natural communities, nutrient
278 cross-feeding can alter gene expression patterns to adapt each species to a syntrophic lifestyle (23–26). In
279 some cases, the lifestyles exhibited within a mutualism might not even be possible during growth in
280 isolation. For example, in synthetic communities that pair the sulfate-reducer *Desulfovibrio vulgaris* with
281 the methanogen *Methanococcus maripaludis*, the methanogen consumes H₂ to maintain low partial
282 pressures that permit the sulfate reducer to adopt a fermentative lifestyle that would otherwise be
283 thermodynamically infeasible (5). Similarly, in an experimental *Geobacter* coculture, direct electron
284 transfer from *Geobacter metallireducens* to *Geobacter sulfurreducens* makes ethanol fermentation by *G.*
285 *metallireducens* thermodynamically possible (7).

286 Similar to our mutualistic system, the mutualism between *D. vulgaris* and *M. maripaludis*
287 represents a facultative mutualism, at least in the short term prior to evolutionary erosion of independent
288 lifestyles (27). For mutualistic relationships to persist between partners that are conditionally capable of a
289 free-living lifestyle, the relationship must exhibit resilience, or the ability to recover its function after a
290 disturbance (28). One important resilience factor is the activation of regulatory networks that allow for
291 microbes to quickly respond to environmental perturbations. Whereas flexible gene expression is useful
292 for an individual microbe's survival, excessive flexibility can sometimes lead to community collapse
293 between mutualists in a fluctuating environment (29, 30). In the aforementioned coculture of *D. vulgaris*
294 and *M. maripaludis*, it was shown that alternating between coculture and monoculture conditions, which
295 require different metabolic lifestyles, resulted in community collapse (29, 30). Surprisingly, community
296 collapse could be avoided by mutations that disrupted the *D. vulgaris* regulatory response needed to adapt
297 cells for optimal growth rates in monoculture (29). Disruption of this regulatory response resulted in a
298 heterogeneous *D. vulgaris* population, ensuring that a subpopulation would be primed for immediate
299 mutualistic growth upon transition between growth conditions (30). In our system, the *E. coli* nitrogen
300 starvation regulatory network was specifically activated by coculturing with *R. palustris* and was
301 important for coculture stability. It is currently unclear if transitioning *E. coli* between monoculture and

302 coculture conditions would result in similar community collapse or whether the NtrC-regulated network
303 would adjust rapidly enough to meet the demands of each condition.

304 Nutrient starvation and other stress responses are widely conserved in diverse microbes and are
305 primarily regarded as necessary for an individual's survival in nutrient-limited environments (31–34).
306 Many microbial communities are composed of primarily slow-growing or even non-growing
307 subpopulations (35–37). However, lack of microbial growth in these communities does not imply
308 cessation of cross-feeding, as bacteria often carry out growth-independent maintenance processes at slow
309 rates (38), and such activities can be coupled to cross-feeding (11). Our findings suggest that nutrient
310 starvation and perhaps other stress responses can help stabilize microbial cross-feeding interactions,
311 especially at low nutrient cross-feeding levels. The extent to which specific starvation or stress responses
312 are active in diverse mutualistic relationships remains unclear, yet likely depends on the environmental
313 context. Together our results highlight the important role that alternate physiological states, including
314 stress responses, can play in establishing and maintaining mutualistic cross-feeding relationships.

315

316 **Materials and Methods**

317 **Strains and growth conditions.** Strains, plasmids, and primers are listed in Table S1. All *R. palustris*
318 strains contained $\Delta uppE$ and $\Delta hupS$ mutations to facilitate accurate colony forming unit (CFU)
319 measurements by preventing cell aggregation (39) and to prevent H₂ uptake, respectively. *E. coli* was
320 cultivated on Luria-Burtani (LB) agar and *R. palustris* on defined mineral (PM) (40) agar with 10 mM
321 succinate. (NH₄)₂SO₄ was omitted from PM agar for determining *R. palustris* CFUs. Monocultures and
322 cocultures were grown in 10 mL of defined M9-derived coculture medium (MDC) (10) in 27-mL
323 anaerobic test tubes under 100% N₂ as described (10). MDC was supplemented with cation solution (1 %
324 v/v; 100 mM MgSO₄ and 10 mM CaCl₂) and glucose (25 mM), unless indicated otherwise. All cultures
325 were grown at 30°C laying horizontally under a 60 W incandescent bulb with shaking at 150 rpm. Starter
326 cocultures were inoculated with 200 μL MDC containing a suspension of a single colony of each species.
327 Test cocultures and serial transfers were inoculated using a 1% dilution from starter cocultures. For

328 experiments requiring a starting species ratio of 1:1, *E. coli* and *R. palustris* starter monocultures were
329 grown to equivalent cell densities, and inoculated at equal volumes. For harvesting RNA and protein, 100
330 mL cultures were grown shaking in 260-mL serum vials with 25 mM glucose and 10 mM cation solution.
331 *R. palustris* monocultures were further supplemented with 15 mM sodium bicarbonate and an organic
332 acid mixture containing 7.8 mM sodium acetate, 8.7 mM disodium succinate, 1.5 mM sodium lactate, 0.3
333 mM sodium formate, and 6.7mM ethanol as carbon sources. *E. coli* monocultures were supplemented
334 with 2.5 mM NH₄Cl as a nitrogen source. Kanamycin was added to a final concentration of 30 µg/ml for
335 *E. coli* where appropriate. Chloramphenicol was added to a final concentration of 5 µg/ml for both *R.*
336 *palustris* and *E. coli* where appropriate.

337 **Generation of *E. coli* mutants.** P1 transduction (41) was used to introduce deletions from Keio
338 collection strains into MG1655. The genotype of kanamycin-resistant colonies was confirmed by PCR
339 and sequencing.

340 **Analytical procedures.** Cell density was assayed by optical density at 660 nm (OD₆₆₀) using a Genesys
341 20 visible spectrophotometer (Thermo-Fisher, Waltham, MA, USA). Growth curve readings were taken
342 in culture tubes without sampling (i.e., tube OD₆₆₀). Specific growth rates were determined using readings
343 between 0.1-1.0 OD₆₆₀ where there is linear correlation between cell density and OD₆₆₀. Final OD₆₆₀
344 measurements were taken in cuvettes and samples were diluted into the linear range as necessary.
345 Glucose, organic acids, formate and ethanol were quantified using a Shimadzu high-performance liquid
346 chromatograph (HPLC) as described (42).

347 **Sample collection for transcriptomics and proteomics.** Monocultures and cocultures were grown in
348 100-mL volumes to late exponential phase and immediately chilled in an ice-water bath. A 1-mL sample
349 was collected for protein quantification using a Pierce BCA Protein Assay Kit as per the manufacturer's
350 protocol. A 5-ml sample was removed for RNA extraction and 90 ml was used for proteomic analysis. All
351 samples were centrifuged at 4°C to pellet cells, frozen in liquid N₂, and stored at -80°C until processing.

352 **RNA-seq.** Total RNA was isolated from late exponential cell pellets using the RNeasy kit (Qiagen,
353 Valencia, CA, USA) as per the manufacturer's protocol. In order to calculate baseline expression levels,

354 RNA sequencing reads resulting from monoculture were mapped to their corresponding reference genome
355 (*E. coli* str. K-12 substr. MG1655 (43), NCBI RefSeq: NC_000913.3; *R. palustris* CGA0009 (44), NCBI
356 RefSeq: NC_005296.1) using the Tuxedo protocol for RNA expression analysis (45) (Workflow
357 deposited at <https://github.com/behring/Task3/RNASeq>). Specifically, split-reads were aligned to the
358 reference genome with Tophat2 (v.2.1.0) (46) and Bowtie2 (v.2.1.0) (47). Following mapping, transcripts
359 were assembled with cufflinks (v.2.2.0) (48), and differential expression was identified with the cufflinks
360 tool, cuffdiff (v.2.2.0). To assure that crossmapping of homologous sequencing reads would not
361 complicate expression analysis from the co-culture experiments, monoculture reads were additionally
362 mapped as described to the opposing genome. As all potential crossmapping was confined to residual
363 rRNA reads, these regions were excluded from the analysis and the co-culture RNA-seq reads were
364 analyzed by mapping the sequenced reads to both reference genomes with no further correction.

365 **Analysis by LC-MS/MS.** Mass spectrometry was performed at the Mass Spectrometry and Proteomics
366 Research Laboratory (MSPRL), FAS Division of Science, at Harvard University. Samples were
367 individually labeled with tandem mass tag (TMT) 10-plex reagents according to the manufacturer's
368 protocol (ThermoFisher Scientific) and mixed. The mixed sample was dried in a speedvac and re-diluted
369 with Buffer A (0.1 % formic acid in water) for injection for HPLC runs. The sample was submitted for a
370 single liquid chromatography coupled to tandem mass spectrometry (LC-MS/MS) experiment which was
371 performed on a LTQ Orbitrap Elite (ThermoFisher Scientific) equipped with Waters (Milford, MA)
372 NanoAcquity HPLC pump. Peptides were separated onto a 100 μm inner diameter microcapillary trapping
373 column packed first with approximately 5 cm of C18 Reprosil resin (5 μm , 100 \AA , Dr. Maisch GmbH,
374 Germany) followed by analytical column ~20 cm of Reprosil resin (1.8 μm , 200 \AA , Dr. Maisch GmbH,
375 Germany). Separation was achieved through applying a gradient from 5–27% ACN in 0.1% formic acid
376 over 90 min at 200 nl min^{-1} . Electrospray ionization was enabled through applying a voltage of 1.8 kV
377 using a home-made electrode junction at the end of the microcapillary column and sprayed from fused
378 silica pico tips (New Objective, MA). The LTQ Orbitrap Elite was operated in data-dependent mode for
379 the mass spectrometry methods. The mass spectrometry survey scan was performed in the Orbitrap in the

380 range of 395 –1,800 m/z at a resolution of 6×10^4 , followed by the selection of the twenty most intense
381 ions (TOP20) for CID-MS2 fragmentation in the ion trap using a precursor isolation width window of 2
382 m/z, AGC setting of 10,000, and a maximum ion accumulation of 200 ms. Singly charged ion species
383 were not subjected to CID fragmentation. Normalized collision energy was set to 35 V and an activation
384 time of 10 ms. Ions in a 10 ppm m/z window around ions selected for MS2 were excluded from further
385 selection for fragmentation for 60 s. The same TOP20 ions were subjected to HCD MS2 event in Orbitrap
386 part of the instrument. The fragment ion isolation width was set to 0.7 m/z, AGC was set to 50,000, the
387 maximum ion time was 200 ms, normalized collision energy was set to 27V and an activation time of 1
388 ms for each HCD MS2 scan.

389 **Mass spectrometry data analysis.** Raw data were submitted for analysis in MaxQuant 1.5.6.5 (13).
390 Assignment of MS/MS spectra was performed by searching the data against a protein sequence database
391 including all entries from the *E. coli* MG1655 proteome (49), the *R. palustris* CGA009 proteome (44),
392 and other known contaminants such as human keratins and common lab contaminants. MaxQuant
393 searches were performed using a 20 ppm precursor ion tolerance with a requirement that each peptide had
394 N termini consistent with trypsin protease cleavage, allowing up to two missed cleavage sites. 10-plex
395 TMT tags on peptide amino termini and lysine residues were set as static modifications while methionine
396 oxidation and deamidation of asparagine and glutamine residues were set as variable modifications. MS2
397 spectra were assigned with a false discovery rate (FDR) of 1% at the protein level by target-decoy
398 database search. Per-peptide reporter ion intensities were exported from MaxQuant (evidence.txt). Only
399 peptides with a parent ion fraction greater than or equal to 0.5 were used for subsequent analysis (6063 of
400 9987 peptides). Intensities were calculated as the sum of peptide intensities. Ratios between conditions
401 were computed at the peptide level, and the protein ratio was computed as the mean of peptide ratios. All
402 ratios were normalized by dividing by the median value for proteins from the same species. Ratio
403 significance for coculture conditions at an FDR of 1% was computed by determining the ratio r at which
404 99% of genes have ratio less than r when comparing biological replicate monocultures.

405

406 **Expression of *E. coli amtB* in coculture.** The ASKA collection (50) plasmid harboring an IPTG-
407 inducible copy of *amtB* (pCA24N *amtB*) was purified from strain JW0441-AM and introduced by
408 electroporation into WT *E. coli* and Δ NtrC. Cocultures were inoculated with either single colonies of each
409 species or at a 1:1 starting species ratio, as indicated in the figure legends. IPTG and 5 μ g/ml
410 chloramphenicol were supplemented to cocultures to induce *E. coli amtB* expression in cocultures and
411 maintain the plasmid, respectively.

412

413 **Acknowledgments**

414 We thank B. A. Budnik and R. A. Robins (Harvard MSPRL) for assistance with mass spectrometry.

415 We thank P. L. Foster for providing the Keio and ASKA *E. coli* collections. This work was supported in
416 part by the U.S. Department of Energy, Office of Science, Office of Biological and Environmental
417 Research, under Award Number DE-SC0008131, by the U.S. Army Research Office, grant W911NF-14-
418 1-0411, by a National Institutes of Health National Service Award F32GM123703 to M. G. Behringer,
419 and by the Indiana University College of Arts and Sciences.

420

421 **References**

- 422 1. **Seth EC, Taga ME.** 2014. Nutrient cross-feeding in the microbial world. *Front. Microbiol.* **5**:1–6.
- 423 2. **Hammer ND, Cassat JE, Noto MJ, Lojek LJ, Chadha AD, Schmitz JE, Creech CB, Skaar**
424 **EP.** 2014. Inter- and Intraspecies Metabolite Exchange Promotes Virulence of Antibiotic-Resistant
425 *Staphylococcus aureus*. *Cell Host Microbe* **16**:531–537.
- 426 3. **Ramsey MM, Rumbaugh KP, Whiteley M.** 2011. Metabolite cross-feeding enhances virulence
427 in a model polymicrobial infection. *PLoS Pathog.* **7**:1–8.
- 428 4. **Iannotti EL, Kafkewit D, Wolin MJ, Bryant MP.** 1973. Glucose Fermentation Products of
429 *Ruminococcus-Albus* Grown in Continuous Culture with *Vibrio-Succinogenes* - Changes Caused
430 by Interspecies Transfer of H₂. *J. Bacteriol.* **114**:1231–1240.
- 431 5. **Stolyar S, Van Dien S, Hillesland KL, Pinel N, Lie TJ, Leigh J a, Stahl D a.** 2007. Metabolic

- 432 modeling of a mutualistic microbial community. *Mol. Syst. Biol.* **3**:92.
- 433 6. **Walker CB, Redding-Johanson AM, Baidoo EE, Rajeev L, He Z, Hendrickson EL,**
434 **Joachimiak MP, Stolyar S, Arkin AP, Leigh J a, Zhou J, Keasling JD, Mukhopadhyay A,**
435 **Stahl D a.** 2012. Functional responses of methanogenic archaea to syntrophic growth. *ISME J.*
436 **6**:2045–2055.
- 437 7. **Summers ZM, Fogarty HE, Leang C, Franks AE, Malvankar NS, Lovley DR.** 2010. Direct
438 exchange of electrons within aggregates of an evolved syntrophic coculture of anaerobic bacteria.
439 *Science* **330**:1413–5.
- 440 8. **Widder S, Allen RJ, Pfeiffer T, Curtis TP, Wiuf C, Sloan WT, Cordero OX, Brown SP,**
441 **Momeni B, Shou W, Kettle H, Flint HJ, Haas AF, Laroche B, Kreft J.** 2016. Challenges in
442 microbial ecology: building predictive understanding of community function and dynamics. *ISME*
443 *J* **10**:2557–2568.
- 444 9. **Lindemann SR, Bernstein HC, Song H-S, Fredrickson JK, Fields MW, Shou W, Johnson**
445 **DR, Beliaev AS.** 2016. Engineering microbial consortia for controllable outputs. *ISME J.*
446 **10**:2077–2084.
- 447 10. **LaSarre B, McCully AL, Lennon JT, McKinlay JB.** 2017. Microbial mutualism dynamics
448 governed by dose-dependent toxicity of cross-fed nutrients. *ISME J* **11**:337–348.
- 449 11. **McCully AL, LaSarre B, McKinlay JB.** 2017. Growth-independent cross-feeding modifies
450 boundaries for coexistence in a bacterial mutualism. *Environ. Microbiol.*
- 451 12. **McCully AL, LaSarre B, McKinlay JB.** 2017. Recipient-biased competition for an
452 intracellularly generated cross-fed nutrient is required for coexistence of microbial mutualists.
453 *MBio* **8**:e01620-17.
- 454 13. **Cox J, Mann M.** 2008. MaxQuant enables high peptide identification rates, individualized p.p.b.-
455 range mass accuracies and proteome-wide protein quantification. *Nat. Biotechnol.* **26**:1367–1372.
- 456 14. **Jozefczuk S, Klie S, Catchpole G, Szymanski J, Cuadros-Inostroza A, Steinhauser D, Selbig**
457 **J, Willmitzer L.** 2010. Metabolomic and transcriptomic stress response of *Escherichia coli*. *Mol.*

- 458 Syst. Biol. **6**:1–16.
- 459 15. **Lessard IAD, Pratt SD, Mccafferty DG, Bussiere DE, Hutchins C, Wanner BL, Katz L,**
460 **Walsh CT.** 1998. Homologs of the vancomycin resistance D-Ala-D-Ala dipeptidase VanX in
461 *Streptomyces toyocaensis*, *Escherichia coli* and *Synechocystis* □: attributes of catalytic efficiency
462, stereoselectivity and regulation with implications for function. *Chem. Biol.* **5**.
- 463 16. **Kim KS, Pelton JG, Inwood WB, Andersen U, Kustu S, Wemmer DE.** 2010. The Rut pathway
464 for pyrimidine degradation: Novel chemistry and toxicity problems. *J. Bacteriol.* **192**:4089–4102.
- 465 17. **Caldara M, Charlier D, Cunin R.** 2006. The arginine regulon of *Escherichia coli*: Whole-system
466 transcriptome analysis discovers new genes and provides an integrated view of arginine regulation.
467 *Microbiology* **152**:3343–3354.
- 468 18. **Kashiwagi K, Pistocchi R, Shibuya S, Sugiyama S, Morikawa K, Igarashi K.** 1996.
469 Spermidine-preferential Uptake System in *Escherichia coli*. *J. Biol. Chem.* **271**:12205–12208.
- 470 19. **van Heeswijk WC, Westerhoff H V., Boogerd FC.** 2013. Nitrogen Assimilation in *Escherichia*
471 *coli*: Putting Molecular Data into a Systems Perspective. *Microbiol. Mol. Biol. Rev.* **77**:628–695.
- 472 20. **Zimmer DP, Soupene E, Lee HL, Wendisch VF, Khodursky AB, Peter BJ, Bender RA,**
473 **Kustu S.** 2000. Nitrogen regulatory protein C-controlled genes of *Escherichia coli*: scavenging as
474 a defense against nitrogen limitation. *Proc. Natl. Acad. Sci. U. S. A.* **97**:14674–14679.
- 475 21. **Barney BM, Eberhart LJ, Ohlert JM, Knutson CM, Plunkett MH.** 2015. Gene Deletions
476 Resulting in Increased Nitrogen Release by *Azotobacter vinelandii*: Application of a Novel
477 Nitrogen Biosensor. *Appl. Environ. Microbiol.* **81**:4316–4328.
- 478 22. **Kim M, Zhang Z, Okano H, Yan D, Groisman A, Hwa T.** 2012. Need-based activation of
479 ammonium uptake in *Escherichia coli*. *Mol. Syst. Biol.* **8**:1–10.
- 480 23. **Rosenthal AZ, Matson EG, Eldar A, Leadbetter JR.** 2011. RNA-seq reveals cooperative
481 metabolic interactions between two termite-gut spirochete species in co-culture. *ISME J.* **5**:1133–
482 1142.
- 483 24. **Filkins LM, Graber J a., Olson DG, Dolben EL, Lynd LR, Bhujju S, Toole AO, O’Toole G a.**

- 484 2015. Coculture of *Staphylococcus aureus* with *Pseudomonas aeruginosa* Drives *S. aureus* towards
485 Fermentative Metabolism and Reduced Viability in a Cystic Fibrosis Model. *J. Bacteriol.*
486 **197**:JB.00059-15.
- 487 25. **Men Y, Feil H, VerBerkmoes NC, Shah MB, Johnson DR, Lee PKH, West KA, Zinder SH,**
488 **Andersen GL, Alvarez-Cohen L.** 2012. Sustainable syntrophic growth of *Dehalococcoides*
489 *ethenogenes* strain 195 with *Desulfovibrio vulgaris* Hildenborough and *Methanobacterium*
490 *congolense*: global transcriptomic and proteomic analyses. *ISME J.* **6**:410–421.
- 491 26. **Giannone RJ, Huber H, Karpinets T, Heimerl T, Küper U, Rachel R, Keller M, Hettich RL,**
492 **Podar M.** 2011. Proteomic characterization of cellular and molecular processes that enable the
493 *Nanoarchaeum equitans-ignicoccus hospitalis* relationship. *PLoS One* **6**.
- 494 27. **Hillesland KL, Lim S, Flowers JJ, Turkarslan S, Pinel N, Zane GM, Elliott N, Qin Y, Wu L,**
495 **Baliga NS, Zhou J, Wall JD, Stahl DA.** 2014. Erosion of functional independence early in the
496 evolution of a microbial mutualism. *Proc. Natl. Acad. Sci.* **111**:14822–14827.
- 497 28. **Song HS, Renslow RS, Fredrickson JK, Lindemann SR.** 2015. Integrating ecological and
498 engineering concepts of resilience in microbial communities. *Front. Microbiol.* **6**:1–7.
- 499 29. **Turkarslan S, Raman A V, Thompson AW, Arens CE, Gillespie MA, von Netzer F,**
500 **Hillesland KL, Stolyar S, López García de Lomana A, Reiss DJ, Gorman Lewis D, Zane**
501 **GM, Ranish JA, Wall JD, Stahl DA, Baliga NS.** 2017. Mechanism for microbial population
502 collapse in a fluctuating resource environment. *Mol. Syst. Biol.* **13**:919.
- 503 30. **Thompson AW, Turkarslan S, Arens CE, López García de Lomana A, Raman A V., Stahl**
504 **DA, Baliga NS.** 2017. Robustness of a model microbial community emerges from population
505 structure among single cells of a clonal population. *Environ. Microbiol.* **19**:3059–3069.
- 506 31. **Kjelleberg S, Albertson N, Flardh K, Holmquist L, Jouper-Jaan A, Marouga R, Ostling J,**
507 **Svenblad B, Weichart D.** 1993. How do non-differentiating bacteria adapt to starvation? *Antonie*
508 *Van Leeuwenhoek* **63**:333–341.
- 509 32. **Shimizu K.** 2013. Regulation Systems of Bacteria such as *Escherichia coli* in Response to

- 510 Nutrient Limitation and Environmental Stresses. *Metabolites* **4**:1–35.
- 511 33. **Barbara S, Resources N, Collins F.** 2007. Microbial Stress-Response Physiology and Its
512 Implications **88**:1386–1394.
- 513 34. **Roszak DB, Colwell RR.** 1987. Survival strategies of bacteria in the natural environment.
514 *Microbiol. Rev.* **51**:365–379.
- 515 35. **Jørgensen BB, Marshall IPG.** 2016. Slow Microbial Life in the Seabed. *Ann. Rev. Mar. Sci.*
516 **8**:311–332.
- 517 36. **Bergkessel M, Basta DW, Newman DK.** 2016. The physiology of growth arrest: uniting
518 molecular and environmental microbiology. *Nat. Rev. Microbiol.* **14**:549–562.
- 519 37. **Lennon JT, Jones SE.** 2011. Microbial seed banks: The ecological and evolutionary implications
520 of dormancy. *Nat. Rev. Microbiol.* **9**:119–130.
- 521 38. **Wanner U, Egli T.** 1990. Dynamics of microbial growth and cell composition in batch culture.
522 *FEMS Microbiol. Rev.* **6**:19–43.
- 523 39. **Fritts RK, LaSarre B, Stoner AM, Posto AL, Mckinlay JB.** 2017. A Rhizobiales-specific
524 unipolar polysaccharide adhesin contributes to *Rhodopseudomonas palustris* biofilm formation
525 across diverse photoheterotrophic conditions **83**:1–14.
- 526 40. **Kim M-K, Harwood CS.** 1991. Regulation of benzoate-CoA ligase in *Rhodopseudomonas*
527 *palustris*. *FEMS Microbiol. Lett.* **83**:199–203.
- 528 41. **Thomason LC, Costantino N, Court DL.** 2007. *E. coli* Genome Manipulation by P1
529 Transduction. *Curr. Protoc. Mol. Biol.* 1.17.1-1.17.8.
- 530 42. **McKinlay JB, Zeikus JG, Vieille C.** 2005. Insights into *Actinobacillus succinogenes*
531 Fermentative Metabolism in a Chemically Defined Growth Medium Insights into *Actinobacillus*
532 *succinogenes* Fermentative Metabolism in a Chemically Defined Growth Medium. *Appl Env.*
533 *Microbiol* **71**:6651–6656.
- 534 43. **Hayashi K, Morooka N, Yamamoto Y, Fujita K, Isono K, Choi S, Ohtsubo E, Baba T,**
535 **Wanner BL, Mori H, Horiuchi T.** 2006. Highly accurate genome sequences of *Escherichia coli*

536 K-12 strains MG1655 and W3110. *Mol. Syst. Biol.* **2**:2006.0007.

537 44. **Larimer FW, Chain P, Hauser L, Lamerdin J, Malfatti S, Do L, Land ML, Pelletier D a,**
538 **Beatty JT, Lang AS, Tabita FR, Gibson JL, Hanson TE, Bobst C, Torres JLTY, Peres C,**
539 **Harrison FH, Gibson J, Harwood CS.** 2004. Complete genome sequence of the metabolically
540 versatile photosynthetic bacterium *Rhodospseudomonas palustris*. *Nat. Biotechnol.* **22**:55–61.

541 45. **Trapnell C, Roberts A, Goff L, Pertea G, Kim D, Kelley DR, Pimentel H, Salzberg SL, Rinn**
542 **JL, Pachter L.** 2012. Differential gene and transcript expression analysis of RNA-seq
543 experiments with TopHat and Cufflinks. *Nat. Protoc.* **7**:562–578.

544 46. **Kim D, Pertea G, Trapnell C, Pimentel H, Kelley R, Salzberg SL.** 2013. TopHat2: accurate
545 alignment of transcriptomes in the presence of insertions, deletions and gene fusions. *Genome*
546 *Biol.* **14**:R36.

547 47. **Langmead B, Salzberg SL.** 2012. Fast gapped-read alignment with Bowtie 2. *Nat. Methods*
548 **9**:357–9.

549 48. **Trapnell C, Williams BA, Pertea G, Mortazavi A, Kwan G, van Baren MJ, Salzberg SL,**
550 **Wold BJ, Pachter L.** 2010. Transcript assembly and quantification by RNA-Seq reveals
551 unannotated transcripts and isoform switching during cell differentiation. *Nat. Biotechnol.* **28**:511–
552 515.

553 49. **The UniProt Consortium.** 2017. UniProt: The universal protein knowledgebase. *Nucleic Acids*
554 *Res.* **45**:D158–D169.

555 50. **Kitagawa M, Ara T, Arifuzzaman M, Ioka-Nakamichi T, Inamoto E, Toyonaga H, Mori H.**
556 2005. Complete set of ORF clones of *Escherichia coli* ASKA library (A complete set of *E. coli* K-
557 12 ORF archive): unique resources for biological research. *DNA Res.* **12**:291–299.

558 51. **Blattner F, Plunkett G I, Bloch C, Perna N, Burland V, Riley M, Collado-Vides J, Glasner J,**
559 **Rode C, Mayhew G, Gregor J, Davis N, Kirkpatrick H, Goeden M, Rose D, Mau B, Shao Y.**
560 1997. The Complete Genome Sequence of *Escherichia coli* K-12. *Science (80-.)*. **2771613**:1453–
561 1462.

562 52. **Baba T, Ara T, Hasegawa M, Takai Y, Okumura Y, Baba M, Datsenko K a, Tomita M,**
563 **Wanner BL, Mori H.** 2006. Construction of Escherichia coli K-12 in-frame, single-gene
564 knockout mutants: the Keio collection. Mol. Syst. Biol. **2**:2006.0008.
565

566 **Figure Legends**567 **Table 1. Selected differentially expressed transcripts in cocultures of *E. coli* and *R. palustris* compared to monocultures**

Species	Gene symbol	Gene description	<i>Rp</i> Nx + <i>Ec</i> WT		<i>Rp</i> NxΔAmtB + <i>Ec</i> WT		<i>Rp</i> ΔAmtB + <i>Ec</i> WT	
			Fold change ^c	FDR adjusted P-value	Fold change	FDR adjusted P-value	Fold change	FDR adjusted P-value
<i>E. coli</i>	rutA ^b	Pyrimidine monooxygenase	114.5 ± 0.0	0.09	108.0 ± 0.0	0.09	118.0 ± 0.1	0.09
	rutC ^b	Aminoacrylate peracid reductase	60.7 ± 0.1	0.01	58.0 ± 0.1	0.01	60.9 ± 0.1	0.01
	ddpX ^{ab}	D-ala dipeptidase	58.3 ± 0.1	0.01	59.9 ± 0.1	0.01	50.1 ± 0.0	0.01
	rutD ^b	Aminoacrylate hydrolase	56.9 ± 0.0	0.01	52.9 ± 0.1	0.01	56.6 ± 0.1	0.01
	rutE ^b	Malonic semialdehyde	48.8 ± 0.1	0.01	44.4 ± 0.1	0.01	48.2 ± 0.1	0.01
	rutF ^b	FMN reductase	45.2 ± 0.1	0.01	40.3 ± 0.1	0.01	45.5 ± 0.1	0.01
	patA ^{ab}	Putrescine aminotransferase	36.3 ± 0.1	0.01	33.6 ± 0.1	0.01	34.4 ± 0.0	0.01
	argT ^{ab}	Lysine/arginine/ornithine binding protein	35.1 ± 0.3	0.01	38.9 ± 0.3	0.01	35.3 ± 0.3	0.01
	rutG ^b	FMN reductase	28.5 ± 0.0	0.01	26.9 ± 0.0	0.01	29.0 ± 0.1	0.01
	ddpA ^{ab}	Probably dipeptide binding periplasmid protein	23.7 ± 0.0	0.01	26.8 ± 0.0	0.01	21.0 ± 0.0	0.01
	amtB ^{ab}	Ammonium transporter	21.3 ± 0.2	0.02	25.0 ± 0.2	0.01	24.1 ± 0.2	0.01
	metE	Methionine biosynthesis	-16.2 ± 0.1	0.03	23.6 ± 0.6	0.03	22.8 ± 0.5	0.02
	fimF	Fimbriae regulatory protein	-16.3 ± 0.0	0.01	18.4 ± 0.0	0.01	20.3 ± 0.1	0.01
	tar	Methyl-accepting chemotaxis protein II	-16.3 ± 0.2	0.01	15.8 ± 0.2	0.02	15.4 ± 0.2	0.01
	purL ^a	Purine biosynthesis	-16.8 ± 0.0	0.03	20.4 ± 0.1	0.02	18.8 ± 0.0	0.02
	flgD	Flagellar basal body rod modification protein	-17.1 ± 0.1	0.02	16.9 ± 0.0	0.01	17.4 ± 0.1	0.01
	ilvL ^a	Isoleucine biosynthesis	-17.4 ± 0.7	0.02	14.9 ± 0.4	0.02	14.2 ± 0.5	0.02
	pgaB	Glucosamine deacetylase	-17.9 ± 0.0	0.02	18.8 ± 0.0	0.03	17.3 ± 0.0	0.04
	ilvC ^a	Isoleucine biosynthesis	-18.0 ± 0.2	0.03	17.1 ± 0.2	0.04	17.6 ± 0.2	0.03
	metK	Methionine biosynthesis	-19.2 ± 0.1	0.03	17.5 ± 0.1	0.03	17.4 ± 0.1	0.04
	tap	Methyl-accepting chemotaxis protein IV	-19.7 ± 0.3	0.01	22.0 ± 0.2	0.01	22.1 ± 0.2	0.01
	flgC	Flagellar basal body	-20.1 ± 0.1	0.05				
	purK ^a	Purine biosynthesis	-20.7 ± 0.1	0.03	25.1 ± 0.1	0.01	21.02 ± 0.05	0.03
	metA	Methionine biosynthesis	-21.0 ± 0.1	0.02	20.6 ± 0.1	0.02	20.8 ± 0.2	0.02
	ilvG ^a	Isoleucine biosynthesis	-22.1 ± 0.1	0.01	19.3 ± 0.1	0.03	22.14 ± 0.07	0.01
	metF	Methionine biosynthesis	-23.3 ± 0.1	0.01	22.5 ± 0.1	0.01	17.62 ± 0.38	0.03
nadB	Aspartate oxidase	-24.3 ± 0.0	0.08	29.1 ± 0.1	0.05	23.74 ± 0.01	0.07	
<i>R. palustris</i>	RPA1206 ^a	Aldehyde dehydrogenase	36.0 ± 0.9	0.02			62.4 ± 0.4	0.01
	RPA1205 ^a	Putative alcohol dehydrogenase	32.8 ± 0.5	0.02			28.6 ± 0.4	0.01
	RPA0538	Putative porin	31.6 ± 2.3	0.03				
	RPA1009 ^a	Possible cytochrome P450	10.4 ± 0.8	0.03				
	RPA3101 ^a	Unknown	9.4 ± 0.3	0.03			10.3 ± 0.3	0.04
	RPA4045 ^a	Putative aa ABC transport	8.8 ± 0.4	0.02				
	RPA3100	Unknown	7.8 ± 0.2	0.02				
	RPA1010	Beta-lactamase-like	7.7 ± 0.4	0.04				
	RPA4020 ^a	Putative aa ABC transport permease	7.7 ± 0.2	0.02				
	RPA1204	Unknown	7.4 ± 0.1	0.02			7.4 ± 0.1	0.03
	RPA2376	Unknown	-6.9 ± 0.1	0.04	15.4 ± 0.2	0.04	9.0 ± 0.2	0.03
	RPA2142	Putative fatty acid CoA ligase	-7.3 ± 0.1	0.03				
	RPA2377	Unknown	-8.4 ± 0.2	0.02	16.4 ± 0.6	0.05	7.3 ± 0.1	0.02
	RPA2379	Probable acetyltransferase	-8.5 ± 0.3	0.02				

RPA2390	Possible Rhizobactin siderophore biosynthesis	-9.6 ± 0.2	0.06	22.8 ± 0.2	0.05	16.8 ± 0.5	0.03
RPA1260 ^a	Universal stress protein	-10.5 ± 0.0	0.02			7.2 ± 0.0	0.07
RPA2380	Possible tonB dep iron siderophore	-11.4 ± 0.6	0.03	17.1 ± 0.1	0.06	18.4 ± 0.2	0.01
RPA1259	Putative cation-transporting P-type ATPase	-11.6 ± 0.4	0.02			10.6 ± 0.0	0.06
RPA2378 ^a	Putative TonB-dep receptor	-13.1 ± 0.1	0.03	24.1 ± 0.3	0.06	17.5 ± 0.3	0.02

568 Genes shown in table were directly or indirectly mentioned in the text. For a full list of differentially-expressed genes, see Supplementary Data.

569 ^a Genes were also identified as differentially expressed proteins in coculture (Table 2)

570 ^b Gene is transcriptionally activated by *E. coli* NtrC during nitrogen limitation

571 ^c Fold-change values represent mean ± SD. Positive values indicate gene was upregulated in coculture. Negative values indicate gene was
572 downregulated in coculture. Initial cutoff was set to a log₂ value of 2 in at least 2 of 3 biological replicates. For a complete list of all differentially
573 regulated transcripts, refer to supplementary data. Differential expression was determined with the Cufflinks tool cuffdiff (v.2.2.0) (45)

574 **Table 2. Selected differentially expressed proteins in cocultures of *E. coli* and *R. palustris* compared**
575 **to monocultures**

Species	Gene Symbol	Gene Description	Rp Nx + Ec WT	Rp NxΔAmtB + Ec WT
			Normalized Relative Protein Intensity ^c	Normalized Rela Protein Intensit
<i>E. coli</i>	argT ^{ab}	Lysine/arginine/ornithine binding protein	10.9	11.1
	ddpA ^{ab}	D-ala dipeptide permease	5.8	7.2
	gss	Bifunctional glutathionylspermidine synthetase/amidase	4.5	4.7
	tktB	Transketolase	4.1	5.5
	potF ^{ab}	Putrescine-binding periplasmic protein	3.8	4.2
	modA	Molybdate-binding periplasmic protein	3.8	4.0
	gabD ^{ab}	Succinate-semialdehyde dehydrogenase	3.7	4.8
	dapB	4-hydroxy-tetrahydrodipicolinate reductase	3.6	2.8
	talA	Transaldolase A	3.6	4.2
	amtB ^{ab}	NH4 ⁺ Transporter	3.5	3.5
	asnS	Asparagine biosynthesis	-2.1	-1.9
	serA	Serine biosynthesis	-2.1	-2.5
	secE	Protein translocase subunit	-2.1	-1.8
	glf	LPS biosynthesis	-2.1	-1.9
	yjiM	Putative dehydratase	-2.2	-1.9
	sstT	Serine/threonine transporter	-2.2	-2.4
	rmlA1	Carbohydrate biosynthesis	-2.3	-2.1
	ompF	Outer membrane protein	-2.3	-2.3
	ribE	Riboflavin biosynthesis	-2.3	-1.7
	secY	Protein translocase subunit	-2.6	-2.0
glyA	Glycine biosynthesis	-3.2	-3.0	
purE ^a	Purine biosynthesis	-3.3	-3.6	
yqjI	Transcriptional regulator	-3.6	-3.0	
asnA	Aspartate-ammonia ligase	-6.4	-3.8	
<i>R. palustris</i>	RPA1206 ^a	Aldehyde dehydrogenase	10.0	
	RPA1205 ^a	Putative alcohol dehydrogenase	7.8	1.2
	RPA3101 ^a	Unknown	7.1	1.5
	RPA3093	ABC transporter urea/short-chain binding protein	4.8	1.6
	RPA3297	ABC transporter urea/short-chain binding protein	4.7	1.5
	RPA4019	Putative aa ABC transporter system substrate-binding protein	3.9	1.4
	RPA4045 ^a	Putative aa ABC transport	3.3	1.4
	RPA1009 ^a	Possible cytochrome P450	3.2	1.3
	RPA1748	Putative branched-chain amino acid transport system substrate-binding protein	-2.1	-1.4
	RPA2378 ^a	Putative tonB-dependent receptor protein	-2.1	-1.2
	RPA2124	TonB dependent iron siderophore receptor	-2.3	-1.5
	RPA1260 ^a	Universal stress protein	-2.5	-1.5
	RPA2050	Unknown	-2.7	-1.6
	RPA3669	Putative ABC transporter periplasmic solute-binding protein precursor	-2.8	-1.1
	RPA2120	Periplasmic binding protein	-6.0	-1.6

576
577 Proteins shown in table were directly or indirectly mentioned in the text. For a full list of differentially-
578 expressed proteins, see Supplementary Data.

579 ^a Genes were also identified as differentially expressed transcripts in coculture (Table 1)

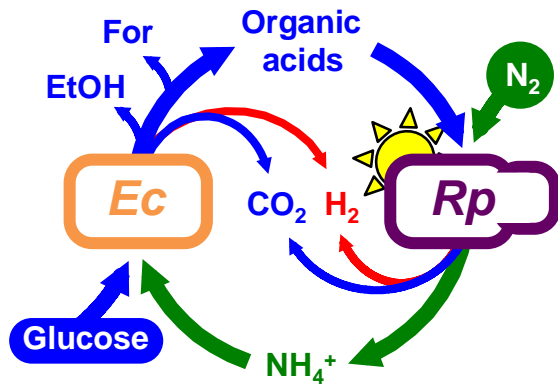
580 ^b Gene is transcriptionally activated by *E. coli* NtrC

581 Values represent mean normalized relative protein intensity for either two^c or one^d biological replicate.

582 Positive values indicate gene was upregulated in coculture. Negative values indicate gene was

583 downregulated in coculture.

584



585

586 **FIG 1. Bidirectional cross-feeding of carbon and nitrogen in an anaerobic bacterial mutualism**

587 **between fermentative *Escherichia coli* (*Ec*) and phototrophic *Rhodospseudomonas palustris* (*Rp*).** *E.*

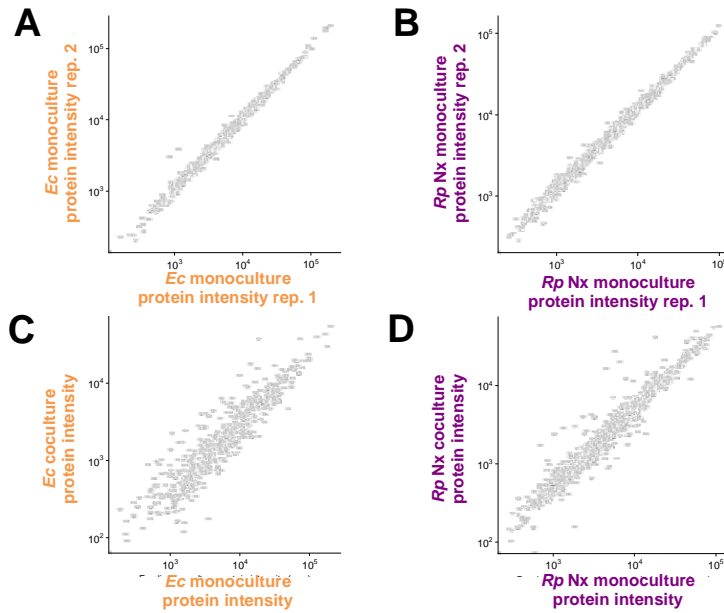
588 *coli* anaerobically ferments glucose into excreted organic acids that *R. palustris* Nx consumes (acetate,

589 lactate and succinate) and other products that *R. palustris* Nx does not consume (formate (For) and

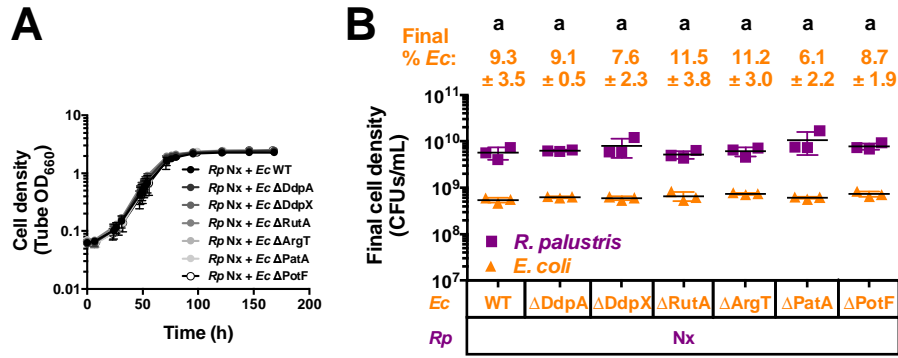
590 ethanol (EtOH)). In return, *R. palustris* Nx constitutively fixes N₂ gas and excretes NH₄⁺, supplying *E.*

591 *coli* with essential nitrogen. *R. palustris* Nx grows photoheterotrophically wherein organic compounds are

592 used for carbon and electrons and light is used for energy.



593
 594 **FIG 2. Coculturing results in altered protein expression patterns in both species, with more**
 595 **differences in WT *E. coli* compared to *R. palustris* Nx.** Protein expression (estimated by LC-
 596 MS/MS intensity) of wild-type *E. coli* (left, **A,C**) and *R. palustris* Nx (right, **B,D**) comparing
 597 protein expression patterns between monoculture biological replicates (rep. 1 versus rep. 2, **A,B**)
 598 and monoculture (average over monoculture replicates) versus coculture (**C,D**).



599

600 **FIG 3. Single deletions of upregulated *E. coli* genes do not impair mutualistic growth with *R.***

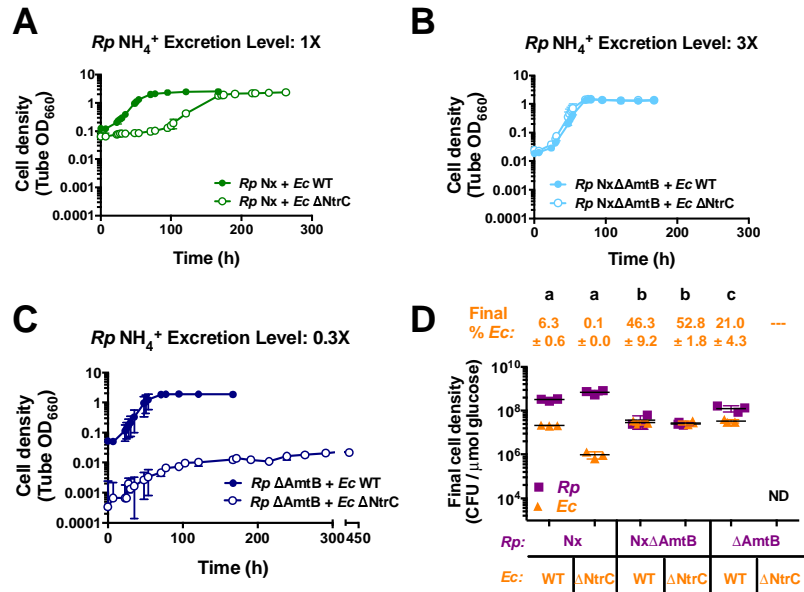
601 ***palustris* Nx.** Growth curves (A) and final cell densities (B) from cocultures pairing *E. coli* (*Ec*) mutants

602 with deletions in highly upregulated genes with *R. palustris* (*Rp*) Nx. Final cell densities were taken at the

603 final time point indicated in (A). Cocultures were started with a 1% inoculum of stationary starter

604 cocultures grown from single colonies. Error bars indicate SD, n=3. Different letters indicate statistical

605 differences, $p < 0.05$, determined by one-way ANOVA with Tukey's multiple comparisons posttest.



606

607 **FIG 4. *R. palustris* NH₄⁺ excretion level affects growth and population trends in cocultures with *E.***

608 ***coli* NtrC.** Growth curves (A,B,C) and final cell densities normalized to glucose consumption (D) from

609 cocultures pairing WT *E. coli* (*Ec*) (filled circles) or ΔNtrC (open circles) with different *R. palustris* (*Rp*)

610 strains that have different NH₄⁺ excretion levels. Final cell densities were taken at the final time point

611 indicated in the respective growth curve, except for cocultures pairing *R. palustris* ΔAmtB with *E. coli*

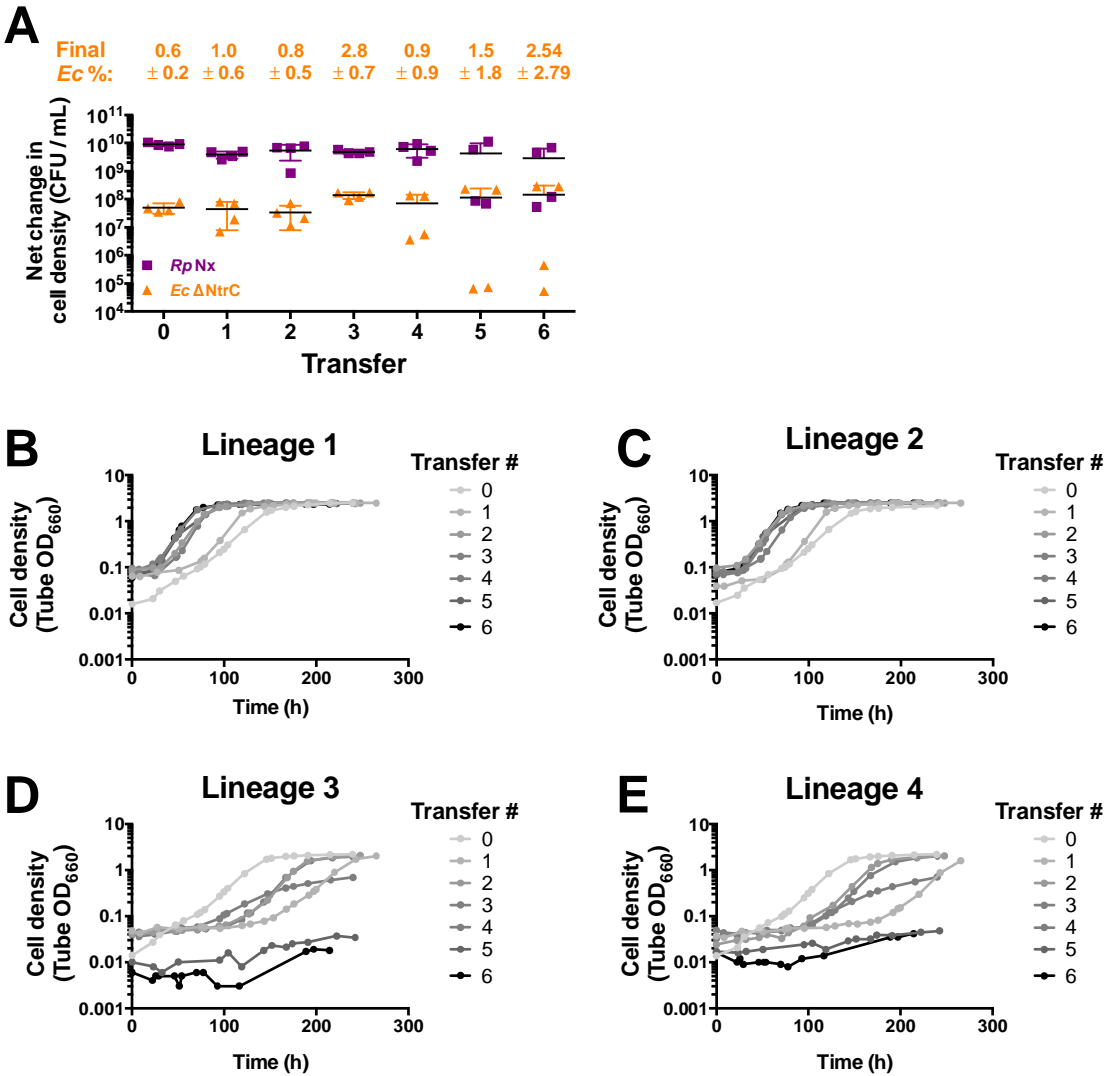
612 ΔNtrC which were sampled at 260 h. Cell densities were normalized to glucose consumed to account for

613 incomplete glucose consumption in cocultures containing *E. coli* ΔNtrC. Cocultures were started with a

614 1% inoculum of stationary starter cocultures grown from single colonies. Error bars indicate SD, n=3.

615 Different letters indicate statistical differences, $p < 0.05$, determined by one-way ANOVA with Tukey's

616 multiple comparisons posttest. ND, not determined.



617

618

FIG 5. Lack of *E. coli* NtrC results in variable coculture growth trends across serial transfers. Net

619

changes in cell densities (A) and replicate growth curves (B-E) of cocultures pairing *E. coli* (*Ec*) Δ NtrC

620

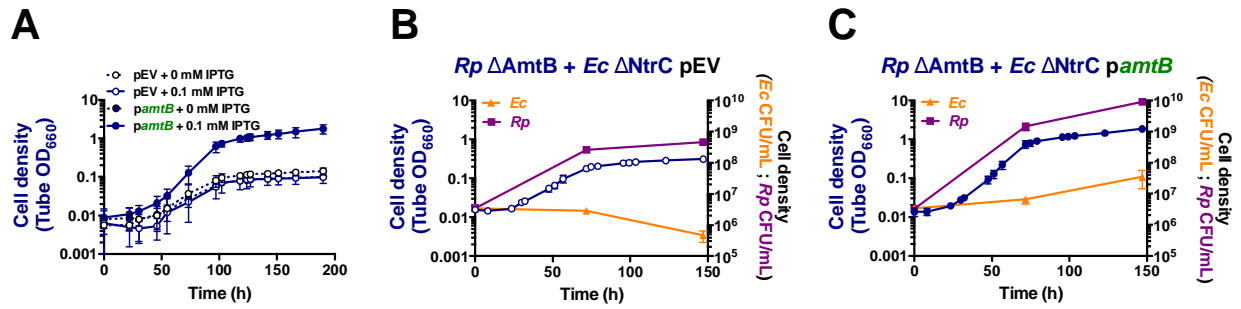
with *R. palustris* (*Rp*) Nx across serial transfers. Cocultures were initially inoculated (Transfer 0) at a 1:1

621

starting species ratios based on CFUs/mL from *R. palustris* and *E. coli* monocultures. A 1% inoculum

622

was used for each serial transfer. Transfers were performed every 10 d. Error bars indicate SD, n=4.



623

624 **FIG 6. Ectopic expression of *amtB* in *E. coli* Δ NtrC permits mutualistic growth with *R. palustris***

625 **Δ AmtB.** Growth curves (A-C) and cell densities for each species (B,C) from cocultures pairing *R.*

626 *palustris* (*Rp*) Δ AmtB with *E. coli* (*Ec*) Δ NtrC harboring a plasmid encoding an IPTG-inducible copy of

627 *amtB* (*pamtB*, filled circles) or an empty vector (*pEV*, open circles). To maintain plasmids, all cocultures

628 were supplemented with 5 μ g/ml chloramphenicol, which is otherwise lethal to *E. coli* but not to *R.*

629 *palustris* (Fig. S6). Cocultures were inoculated with a single colony of each species (A) or at a 1:1

630 starting species ratio based on equivalent CFUs/mL from starter *R. palustris* and *E. coli* monocultures

631 (B,C). 0.1 mM IPTG was added to the cocultures at the initial time point. Error bars indicate SD, n=3.

632 Supplemental

633 Table S1. Strains and plasmids

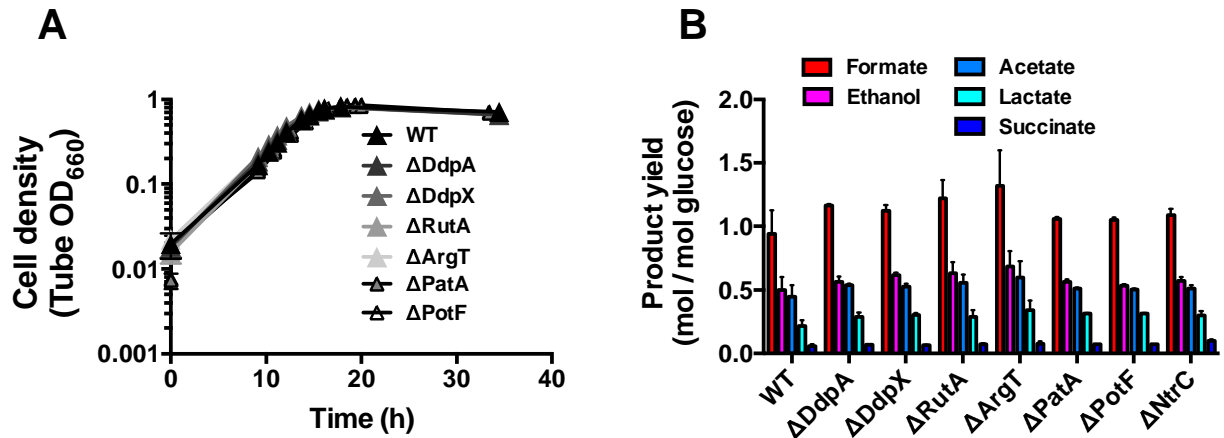
Strain or plasmid	Description or Sequence (5'-3'); <u>Designation</u>	Source or Purpose
<i>R. palustris</i> strains		
CGA009	Wild-type strain; spontaneous Cm ^R derivative of CGA001	(44)
CGA4005	CGA009 $\Delta hupS \Delta uppE nifA^*$; <u>Nx</u>	(10)
CGA4021	CGA4005 $\Delta amtB1 \Delta amtB2$; <u>Nx</u> $\Delta AmtB$	(10)
CGA4026	CGA009 $\Delta hupS \Delta uppE \Delta amtB1 \Delta amtB2$; <u>$\Delta AmtB$</u>	(12)
<i>E. coli</i> strains		
MG1655	Wild-type K12 strain; <u>WT</u>	(51)
K-12 JW1483	Keio collection $\Delta ddpX::Km$	(52)
K-12 JW5240	Keio collection $\Delta ddpA::Km$	(52)
K-12 JW0997	Keio collection $\Delta rutA::Km$	(52)
K-12 JW2307	Keio collection $\Delta argT::Km$	(52)
K-12 JW5510	Keio collection $\Delta patA::Km$	(52)
K-12 JW0838	Keio collection $\Delta potF::Km$	(52)
K-12 JW3840	Keio collection $\Delta ntrC::Km$	(52)
K-12 pCA24N (pASKA)	ASKA collection pCA24N	(50)
MG1655 pCA24N -GFP	ASKA collection pCA24N with gfp removed using NotI digest	This study
K-12 JW0441-AM pASKAamtB	ASKA collection pCA24N-N-His-amtB (gfp minus)	(50)
MG1655 $\Delta DdpX$	MG1655 $\Delta ddpX::Km$; <u>$\Delta DdpX$</u>	This study
MG1655 $\Delta DdpA$	MG1655 $\Delta ddpA::Km$; <u>$\Delta DdpA$</u>	This study
MG1655 $\Delta RutA$	MG1655 $\Delta rutA::Km$; <u>$\Delta RutA$</u>	This study
MG1655 $\Delta ArgT$	MG1655 $\Delta argT::Km$; <u>$\Delta ArgT$</u>	This study
MG1655 $\Delta PatA$	MG1655 $\Delta patA::Km$; <u>$\Delta PatA$</u>	This study
MG1655 $\Delta PotF$	MG1655 $\Delta potF::Km$; <u>$\Delta PotF$</u>	This study
MG1655 $\Delta NtrC$	MG1655 $\Delta ntrC::Km$; <u>$\Delta NtrC$</u>	This study
MG1655 pEV	MG1655 pCA24N; <u>WT pEV</u>	This study
MG1655 $\Delta NtrC$ pEC	MG1655 $\Delta ntrC::Km$ pCA24N; <u>$\Delta NtrC$ pEV</u>	This study
MG1655 <i>pamtB</i>	MG1655 pCA24N-N-His- <i>amtB</i> +; <u>WT <i>pamtB</i></u>	This study
MG1655 $\Delta NtrC$ <i>pamtB</i>	MG1655 $\Delta ntrC::Km$ pCA24N-N-His- <i>amtB</i> +; <u>$\Delta NtrC$ <i>pamtB</i></u>	This study
Plasmids		
pCA24N	Cm ^R ; ASKA collection empty vector with IPTG-inducible promoter	(50)
pCA24N- <i>amtB</i> +	Cm ^R ; ASKA collection vector with IPTG-inducible promoter in front of N-terminal His-tagged <i>amtB</i> gene	(50)
Primers		

ALM47	cggaagcgcagcaattttgt	<i>ddpX</i> upstream flanking region (<i>E. coli</i>)
ALM48	gagcaatgtgggacgaaacg	<i>ddpX</i> downstream flanking region (<i>E. coli</i>)
ALM45	atatcccctggcacacagc	<i>ddpA</i> upstream flanking region (<i>E. coli</i>)
ALM46	ccagcagcgttggcgtaaaata	<i>ddpX</i> downstream flanking region (<i>E. coli</i>)
ALM51	ccgcttgcaacaagcc	<i>rutA</i> upstream flanking region (<i>E. coli</i>)
ALM52	atcagcgcactttgctgc	<i>rutA</i> downstream flanking region (<i>E. coli</i>)
ALM49	gcaaacacacacacaatacacaac	<i>argT</i> upstream flanking region (<i>E. coli</i>)
ALM50	ccatcaggtacagcttcca	<i>argT</i> downstream flanking region (<i>E. coli</i>)
ALM53	tgaaagcgtgctgtaacgc	<i>patA</i> upstream flanking region (<i>E. coli</i>)
ALM54	atcccgattttcgcatcg	<i>patA</i> downstream flanking region (<i>E. coli</i>)
ALM55	ctggccgggagaaagtct	<i>potF</i> upstream flanking region (<i>E. coli</i>)
ALM56	ttacgggttttcgcctgc	<i>potF</i> downstream flanking region (<i>E. coli</i>)
MO 7	caatctttacacacaagctgtgaatc	<i>ntrC</i> upstream flanking region (<i>E. coli</i>)
MO 8	cctgcctatcaggaataaaagg	<i>ntrC</i> downstream flanking region (<i>E. coli</i>)
pCA24N.for	gataacaattcacacagaattcattaagag	ASKA pCA24N upstream into IPTG-inducible promoter upstream of cloned gene
pCA24N.rev	cccattaacatcaccatctaattcaac	ASKA pCA24N downstream into IPTG-inducible promoter upstream of cloned gene

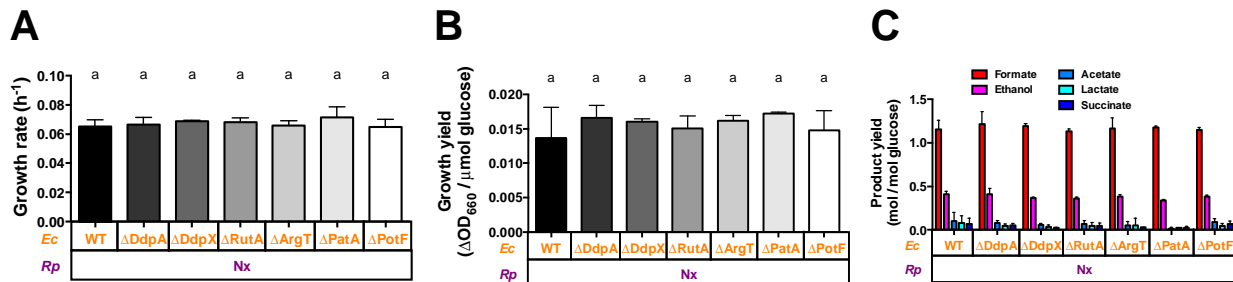
634

635

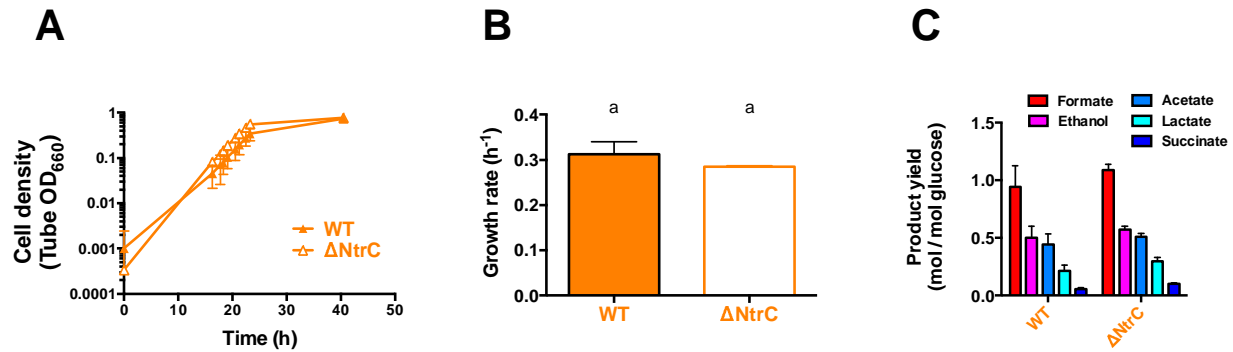
636



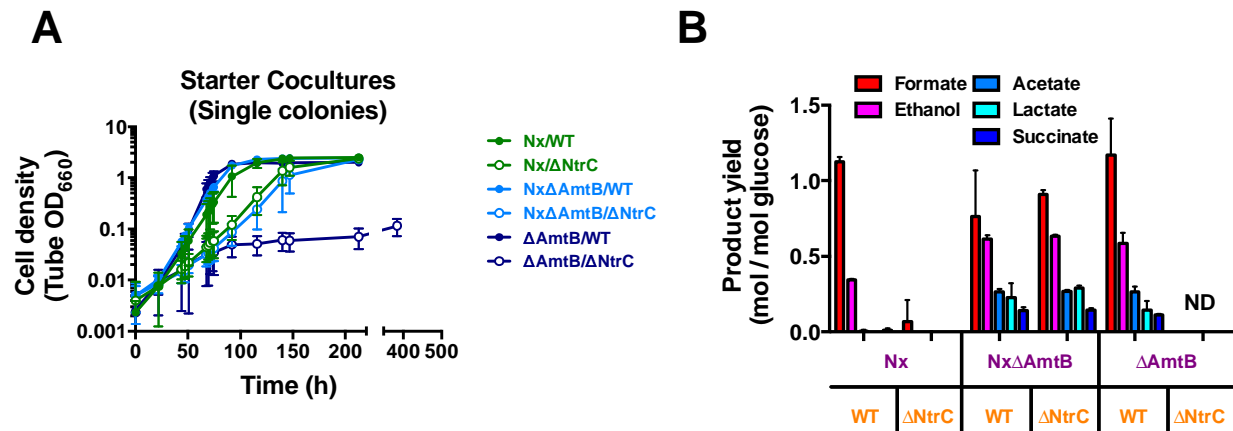
637
 638 **FIG S1. Single deletions of *E. coli* genes that were upregulated in coculture no effect in monoculture**
 639 **with 15 mM NH₄⁺.** Growth curves (A) and product yields (B) from *E. coli* monocultures grown with 15
 640 mM NH₄Cl. Product yields were taken in stationary phase. Error bars indicate SD, n=3.
 641



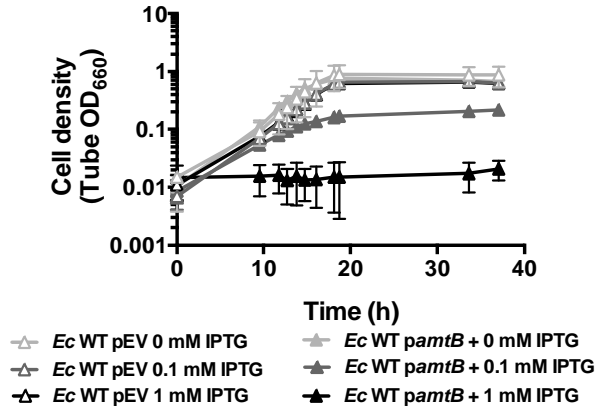
642
 643 **FIG S2. Additional trends from cocultures pairing *R. palustris* Nx with *E. coli* single deletion**
 644 **mutants.** Growth rates (A), growth yields (B), and product yields (C) after a one-week culturing period
 645 from cocultures pairing *E. coli* mutants with deletions in highly upregulated genes with *R. palustris* Nx.
 646 Growth and product yields were taken at the final time point indicated in Fig. 3A. Cocultures were started
 647 with a 1% inoculum of stationary starter cocultures grown from single colonies. Error bars indicate SD,
 648 n=3. Different letters indicate statistical differences, p < 0.05, determined by one-way ANOVA with
 649 Tukey's multiple comparisons posttest.



650
 651 **FIG S3. *E. coli* Δ NtrC growth and metabolic trends are similar to those of WT *E. coli* in**
 652 **monoculture with 15 mM NH_4^+ .** Growth curves (A), growth rate (B) and product yields (C) from WT *E.*
 653 *coli* (filled) or Δ NtrC (open) monocultures grown with 15 mM NH_4Cl . Product yields were taken in
 654 stationary phase. Error bars indicate SD, n=3.
 655



656
 657 **FIG S4. Additional trends from cocultures of *E. coli* Δ NtrC paired with different *R. palustris***
 658 **partners.** Growth curves of starter cocultures inoculated with single colonies of each species (A) and
 659 product yields from test cocultures (B). Product yields were taken at the final time point indicated in the
 660 respective growth curve in Fig. 4. Test cocultures were started with a 1% inoculum of stationary starter
 661 cocultures. Error bars indicate SD, n=3. ND, not determined.



662

663 **FIG S5. Increased *amtB* expression is harmful to *E. coli* in monocultures with 15 mM NH₄⁺.** Growth

664 curves of WT *E. coli* monocultures harboring a plasmid encoding an IPTG-inducible copy of *amtB*

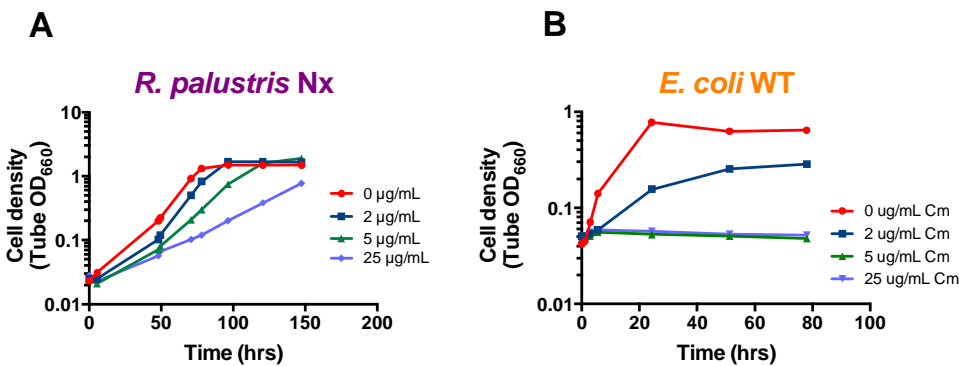
665 (*pamtB*, filled) or empty vector (pEV, open) and grown at different IPTG concentrations. All

666 monocultures were supplemented with 15 mM NH₄Cl and 5 μg/ml chloramphenicol to maintain the

667 plasmid. Cultures were inoculated with a 1% inoculum from stationary monocultures grown in 0 mM

668 IPTG. After inoculation, IPTG was added to the indicated final concentration. Error bars indicate SD,

669 n=3. ND, not determined.



670

671 **FIG S6. Determination of a chloramphenicol concentration to maintain *pamtB* in *E. coli* without**

672 **harming *R. palustris*.** Representative growth curves of *R. palustris* Nx (A) and WT *E. coli* (B) at

673 different concentrations of chloramphenicol. All cultures were grown anaerobically in MDC with a 1%

674 inoculum from stationary monocultures. *R. palustris* Nx was provided 20 mM sodium acetate as a carbon

675 source with a 100% N₂ headspace for nitrogen. WT *E. coli* was provided 25 mM glucose, 10 mM cation

676 solution, and 15 mM NH₄Cl.